Applied Catalysis B: Environmental 126 (2012) 76–85

Contents lists available at SciVerse ScienceDirect

Applied Catalysis B: Environmental

journal homepage: www.elsevier.com/locate/apcatb

Insights towards the influence of Pt features on the photocatalytic activity improvement of TiO_2 by platinisation

J.J. Murcia, J.A. Navío, M.C. Hidalgo*

Instituto de Ciencia de Materiales de Sevilla (ICMS), Consejo Superior de Investigaciones Científicas CSIC - Universidad de Sevilla, Américo Vespucio 49, 41092 Sevilla, Spain

ARTICLE INFO

Article history:
Received 23 April 2012
Received in revised form 6 July 2012
Accepted 16 July 2012
Available online 22 July 2012

Keywords:
Pt-TiO_2
Platinisation
Photodeposition
Photocatalysis
Phenol oxidation
Methyl orange oxidation

ABSTRACT

The influence of Pt features, such as particle size, dispersion, oxidation state and amount of metal, on the improvement of the photoactivity of TiO_2 for phenol and methyl orange degradation was studied.

The size of Pt deposits was precisely controlled by changing deposition time under medium light intensity during the photodeposition, with sizes ranging from 3 to 6 nm. Pt oxidation state was also strongly dependent on the photodeposition time.

Photocatalytic activity results showed that the fraction of metallic platinum (Pt^0) was the crucial factor for the improvement of the activity. When the fraction of Pt^0 was similar, metal deposit size became the dominant parameter influencing the activity.

The influence of the substrate to be degraded (phenol or methyl orange) was also studied.

1. Introduction

The deposition of noble metal nanoparticles on TiO_2 as a means for increasing its photocatalytic efficiency has attracted increasing interest in the last years [1–7]. It is nowadays accepted that the improvement of the photocatalytic activity of TiO_2 by metallisation involves the creation of a Schottky barrier at the metal-TiO_2 interface which serves as a trap for the photogenerated electrons. Thus, the metal nanoparticles act as electrons wells allowing a more efficient separation of the charges, assisting the electron transfer to oxygen or other electron acceptors and thus preventing electron–hole recombination to a higher degree. Increasing the lifetime of the carriers will increase their chances of diffusion to the TiO_2 surface and their participation in the photocatalytic process, promoting in that way the reduction half-reaction considered to be the rate-limiting step in photocatalysis; i.e. reduction of O_2 by conduction band electrons [2,8]. Therefore, the addition of metal nanoparticles, frequently Pt or Au, to TiO_2 generally improves its photocatalytic activity [1,4,5,7].

Lately, Pt-TiO_2 systems have also been reported to exhibit photocatalytic activity in the visible range of the spectrum, where oxidised states of the metal seem to promote this visible response by photoexciting surface plasmons in the metal atom [7,9–11].

In any case, the enhancement of the activity of TiO_2 by its metallisation depends greatly on many factors and this fact makes that many results reported in the literature are apparently contradictories. In the platinisation of TiO_2, the most evident parameter which has a clear influence on the activity is probably the amount of deposited platinum [12,13]. An optimal metal loading is necessary to achieve the desired enhancement of efficiency, usually with Pt contents between 0.5 and 1 wt.%. Thus, an excess of metal would reduce the activity rate because the high amount and proximity of Pt particles could make them act now as recombination centres for the photogenerated charges. Besides, a large amount of metal particles would block active sites on the TiO_2; additionally, the high Pt loading would also produce a decrease in the TiO_2 light absorption by a screen-effect, decreasing in this way the electron–hole pair generation [12,14].

Besides Pt loading, there are other important factors that may influence the degree of improvement in the TiO_2 activity, such as size, dispersion and chemical state of Pt deposits [8,15–17], the substrate to be degraded [18,19] or the nature of the bare TiO_2 [20,21].

Understanding the way in which these different factors affect the activity of TiO_2 is essential for developing new and more efficient metallised photocatalysts. The Pt features in the Pt-TiO_2 systems depend highly on the preparation method used for metal deposition and thus, a careful control of the synthetic route is necessary to obtain the desired properties in amount, size, dispersion and oxidation state of the metallic deposits.

* Corresponding author. Tel.: +34 954489550.
E-mail address: mchidalgo@icmse.csic.es (M.C. Hidalgo).

0926-3373/$ – see front matter © 2012 Elsevier B.V. All rights reserved.
http://dx.doi.org/10.1016/j.apcatb.2012.07.013

In this work, some insights on the influence of the different features of Pt particles on the improvement of the photoefficiency of TiO_2 are given. Additionally, the key parameters of the photodeposition method for precisely tuning Pt particle size and oxidation state are described. Even though photodeposition is a widely used method for Pt addition on TiO_2, apart from pH or kind of sacrificial agent [3,22,23], the influence of the different experimental parameters during the photo-deposition, such as light intensity and deposition time, has been little studied [24]. Studies on TiO_2 platinised by photodeposition often report long irradiation times and high intensity illumination conditions [1,2,5,18,23,25] which probably guarantee total reduction of the metal precursor but cost metal particle growth and agglomeration [26,27].

Thus, the development of preparation methods providing a close control over deposit size, dispersion and chemical state is clearly needed to obtained materials with optimised catalytic properties.

In general terms, it is quite difficult to study the correlation between a single factor in the structure or morphology of a photocatalyst and its activity as this should imply keeping the rest of the material properties constant when varying the studied feature. Otherwise, the influence of synergetic or combination effects cannot be ruled out. The photodeposition method used in this work was performed with a mild intensity light carefully chosen in order to be able to have a better control of the process and the final properties of the platinised materials. Unravelling the effect of Pt features on the improvement of TiO_2 photocatalytic activity is basic for the better understanding of the metallised systems.

The obtained materials were evaluated in the degradation reactions of two very different compounds; i.e. phenol (a well known aromatic contaminant) and methyl orange (widely used dye). Thus, the differences in activity due to the substrate to be degraded were also tested.

Beyond all that has been stated, platinum itself is one of the best catalysts for the conventional thermal oxidation of many different reactions, so the conclusions here obtained can be useful not only in the field of photocatalysis but also in any other field in material science where a careful control of the nanostructure of deposited metals may be needed.

2. Experimental

2.1. Pt-TiO_2 photocatalyts preparation

TiO_2 was prepared by the hydrolysis of titanium tetraisopropoxide (Aldrich, 97%) in isopropanol solution (1.6 M) by the addition of distilled water (volume ratio isopropanol/water 1:1). Afterward, the generated precipitate was filtered and dried at 110 °C overnight. The powders thus obtained were then sulphated by immersion in 1 M sulphuric acid solution for 1 h and calcined at 650 °C for 2 h. This treatment was performed as previous results have shown the positive effect of sulphate pre-treatment on TiO_2 where a synergetic effect between platinisation and sulphation was found resulting in an improved photocatalytic activity [28].

Photodeposition of platinum was carried out over the calcined TiO_2 powder using hexachloroplatinic acid (H_2PtCl_6, Aldrich 99.9%) as metal precursor. Under an inert atmosphere of N_2 to avoid re-oxidation, different suspensions of TiO_2 in distilled water containing isopropanol as sacrificial donor were prepared, adding the appropriate amount of H_2PtCl_6 to obtain two desired nominal platinum loading (0.5 wt.% or 2 wt.% total to TiO_2). Final pH of the suspensions was 3.

After testing photodeposition with different light intensities, a mild intensity of 60 W/m^2 was chosen for this study provided by an Osram Ultra-Vitalux lamp (300 W) with a sun-like radiation spectrum and a main emission line in the UVA range at 365 nm. It was found that this mild photon flux allowed a more precise control of parameters such as metal particle size. A series of samples was then prepared by illuminating the suspensions for different times (15, 30, 60, 120 and 240 min). After photodeposition, the powders were recovered by filtration and dried at 110 °C overnight.

2.2. Characterisation of the Pt-TiO_2 photocatalysts

X-ray diffaction (XRD) patterns were obtained on a Siemens D-501 diffractometer with Ni filter and graphite monochromator using Cu Kα radiation. Crystallite sizes were calculated from the line broadening of the main X-ray diffraction peaks by using the Scherrer equation. Peaks were fitted by using a Voigt function.

BET surface area and porosity measurements were carried out by N_2 adsorption at 77 K using a Micromeritics ASAP 2010 instrument.

Chemical composition and total platinum content of the samples was determined by X-ray fluorescence spectrometry (XRF) in a Panalytical Axios sequential spectrophotometer. XRF measurements were performed onto pressed pellets (sample included in 10 wt.% of wax).

UV–vis spectra were measured on a Varian spectrometer model Cary 100 equipped with an integrating sphere and using $BaSO_4$ as reference. Band-gaps values were calculated from the corresponding Kubelka–Munk functions, $F(R\infty)$, which are proportional to the absorption of radiation, by plotting $(F(R\infty)\cdot h\nu)^{1/2}$ against $h\nu$ [29].

Field Emission Scanning Electron Microscopy (FESEM) images were obtained in a Hitachi S-4800 microscope. Transmission Electron Microscopy (TEM) was performed in a Philips CM200 instrument. In both techniques, samples were dispersed in ethanol using an ultrasonicator and dropped on a carbon grid.

Determination of the metal particle average diameter ($\bar{d}$) in the different samples was accomplished by counting particles in a high number of TEM images from different places of the samples. The following equation was used [30]:

$$\bar{d}(\mathrm{nm}) = \sum d_i \times f_i$$

where d_i is the diameter of the n_i counted particles and f_i is the particle size distribution estimated by:

$$f_i = \frac{n_i}{\sum n_i}$$

where n_i is the number of particles of diameter d_i.

X-ray photoelectron spectroscopy (XPS) study was carried out on a Leybold–Heraeus LHS-10 spectrometer, working with constant pass energy of 50 eV. The spectrometer main chamber, working at a pressure $<2 \times 10^{-9}$ Torr, is equipped with an EA-200 MCD hemispherical electron analyser with a dual X-ray source working with Al Kα ($h\upsilon$ = 1486.6 eV) at 120 W and 30 mA. C 1s signal (284.6 eV) was used as internal energy reference in all the experiments. Samples were outgassed in the prechamber of the instrument at 150 °C up to a pressure $<2 \times 10^{-8}$ Torr to remove chemisorbed water.

2.3. Photocatalytic runs

The evaluation of the photocatalytic activity was performed by using two different model reactions in liquid media; the photooxidation of phenol and methyl orange.

Suspensions of the samples (1 g/l) in phenol solution (50 ppm) or Methyl Orange (50 ppm) were placed in a 400 ml pyrex discontinuous batch reactor enveloped by an aluminium foil and illuminated through a UV-transparent Plexiglas® top window (threshold absorption at 250 nm) by an Osram Ultra-Vitalux lamp (300 W) with sun-like radiation spectrum and a main line in the UVA range at 365 nm. The intensity of the incident UVA light on the solution was determined with a PMA 2200 UVA photometer

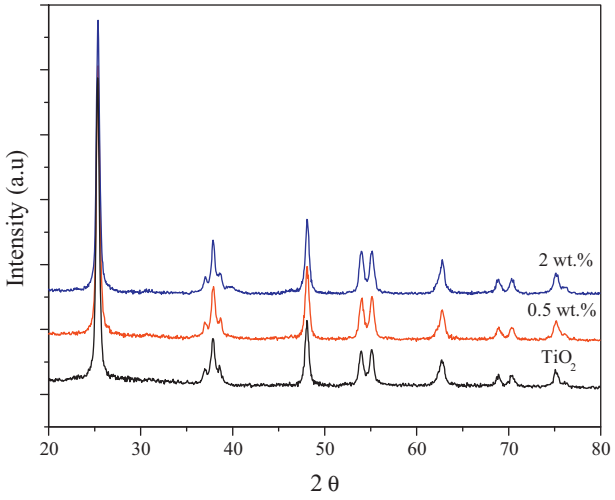

Fig. 1. XRD patterns for TiO_2 and Pt-TiO_2 photocatalysts synthesised at 120 min deposition time with different platinum loading.

(Solar Light Co.) being ca. 140 W/m^2. Magnetic stirring and a constant oxygen flow of 35 l/h as oxidative agent were used to produce a homogeneous suspension of the catalyst in the solution. The pH of the solutions was ca. 6. Prior illumination, catalyst-substrate equilibration was ensured by stirring the suspension 10 min in the dark.

Phenol concentration was followed by HPLC technique (Agilent Technologies 1200) equipped with UV-vis detector using an Elipse XDB-C18 column (5 μm, 4.6 mm × 150 mm). Mobile phase was water/methanol (65:35) at a flow rate of 0.8 ml/min. Methyl orange estimated by UV–vis spectroscopy by following its characteristic band at 460 nm.

Blank experiments were performed in the dark as well as with illumination and no catalyst with both substrates, without observable change in the initial concentration of phenol or methyl orange in any of the cases.

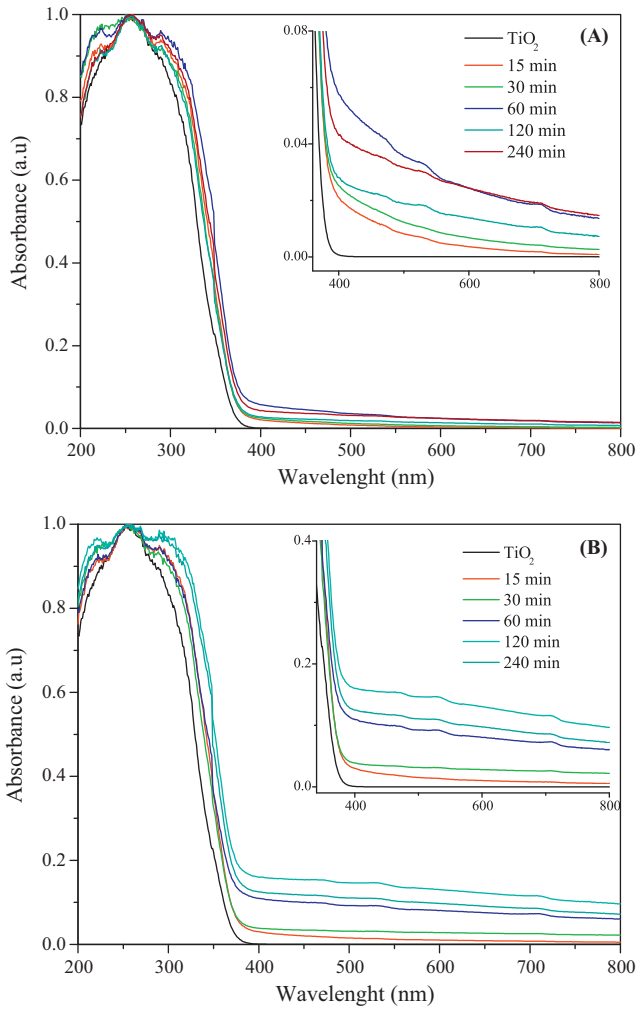

Fig. 2. UV–vis DRS spectra for TiO_2 and Pt-TiO_2 photocatalysts synthesised at the indicated deposition times: (A) 0.5 wt.% and (B) 2 wt.% Pt-TiO_2 samples.

3. Results and discussion

3.1. Structural and chemical characterisation

Crystalline phase composition and degree of crystallinity of the samples were studied by XRD. Fig. 1 shows the XRD patterns for bare TiO_2 and Pt-TiO_2 with 0.5 and 2 wt.% Pt prepared with 120 min deposition time. The spectra of the samples prepared with other deposition times are similar to those in Fig. 1 and are not shown for the sake of brevity. As it can be seen, anatase is the only crystalline phase present for all the samples. The stabilisation of the anatase phase due to the sulphate pre-treatment can be noticed as no peaks of rutile phase are observed for any of the samples after calcination as high as 650 °C [31]. Peaks ascribed to metallic platinum were not observed in any case.

Anatase crystallite sizes of all samples were estimated by the Scherrer equation and the corresponding values are shown in Table 1 . Anatase crystalline size in the pure TiO_2 was 20 nm and this value did not noticeably change with the addition of Pt in any of the samples.

BET surface areas are also shown in Table 1. The original non-platinised TiO_2 has a value of 58 m^2/g. After photodeposition the surface area decreased in a small amount for both metal contents. Then, the area slightly increased up to a deposition time of 60 min and then decreased again for longer deposition times for both series. The initial decrease is surely produced by pore blocking by the metal precursor. With the deposition time the small fluctuations in the surface area could be due to the cleaning of the TiO_2 surface by the photocatalytic process during photodeposition with the corresponding pore liberation.

Pt contents effectively deposited on the samples estimated by XRF are reported in Table 1. As it can be seen, the amount of Pt deposited increased with the deposition time for both Pt contents up to 60 min and then stayed the same or slightly decreased for longer times for both Pt nominal percentages studied. This decrease can be explained due to a certain degree of re-oxidation/desorption of the already reduced metal by the •OH radical formation on the TiO_2 surface as a consequence of the illumination. In any case, the real amount of Pt deposited never reached the nominal content, indicating an incomplete reduction of the precursor.

Impurities were also checked by XRF analysis. In all platinised samples a low amount of Cl^- (between negligible and ca. 0.05%) was detected surely remaining from the platinum precursor (H_2PtCl_6). Sulphur amounts between 0.08 and 0.12% were also found in the samples remaining from the sulphate pre-treatment.

Light absorption properties of the samples were studied by UV–vis spectroscopy. UV–vis diffuse reflectance spectra of TiO_2 and Pt-TiO_2 photocatalysts in the range from 200 to 800 nm for the different deposition times are shown in Fig. 2. The characteristic sharp absorption threshold of TiO_2 around 350 nm was observed in all spectra. Pt-TiO_2 photocatalysts show a higher absorption than TiO_2 throughout the visible range (400–800 nm). The absorption of the

Table 1
Summary of some characterisation results.

	Deposition time (min)	$D_{anatase}$ (nm)	S_{BET} (m^2/g)	wt.% Pt (XRF)	O/Ti (XPS) ratio	%Pt^0 (XPS)
TiO_2	–	20	58	–	1.70	–
	15	22	48	0.23	1.89	n.d.
	30	21	49	0.24	1.88	n.d.
0.5 wt.% Pt-TiO_2	60	21	66	0.34	1.90	n.d.
	120	20	49	0.30	1.91	n.d.
	240	21	45	0.33	1.86	n.d.
	15	21	50	0.61	1.90	13
	30	20	57	0.57	2.00	37
2 wt.% Pt-TiO_2	60	21	62	1.41	1.92	46
	120	21	53	1.25	1.92	63
	240	20	48	1.00	1.99	61

n.d., not determined.

platinised materials in this range increased according to the Pt content (as it can be seen if comparing XRF results and insets in Fig. 2) due to a decrease in reflectivity evidenced by the dark grey colour of these samples.

Band gap energy values for all samples were estimated from the UV–vis absorption measurements. The values were in all cases 3.2 eV without any influence of the Pt content. As it can be noticed in Fig. 2, the same onset of UV absorption of non-platinised and platinised materials implies that they exhibit the same band gap energy with independence of the visible increased absorption shown by the Pt-TiO_2 samples.

3.2. Pt particle size

Morphology, Pt particle size and dispersion of the different samples were studied by FESEM and TEM.

Selected SEM pictures are shown in Fig. 3 for short deposition time (15 min) in Fig. 3A and C and long deposition time (120 min) in Fig. 3B and D, for the samples with 0.5 and 2 wt.% nominal Pt content respectively. Pt deposits appear as particles or aggregation of particles of higher brightness over the round bigger TiO_2 particles. As it can be observed, Pt deposits dispersion decreased with the deposition time for both Pt loadings while the degree of aggregation clearly increased, especially for the 2 wt.% Pt-TiO_2 series.

Metal particle size distribution on the 0.5% Pt-TiO_2 samples prepared with the different deposition times were estimated by counting a high amount of Pt particles in many different TEM pictures from several parts of the samples to achieve representative results. Fig. 4 shows selected TEM pictures of 0.5 wt.% Pt-TiO_2 samples prepared with the different deposition times, where platinum species can be seen as black dots. Histograms for particle size distribution are also depicted beside the corresponding pictures. In agreement with SEM observations, it can be seen that platinum

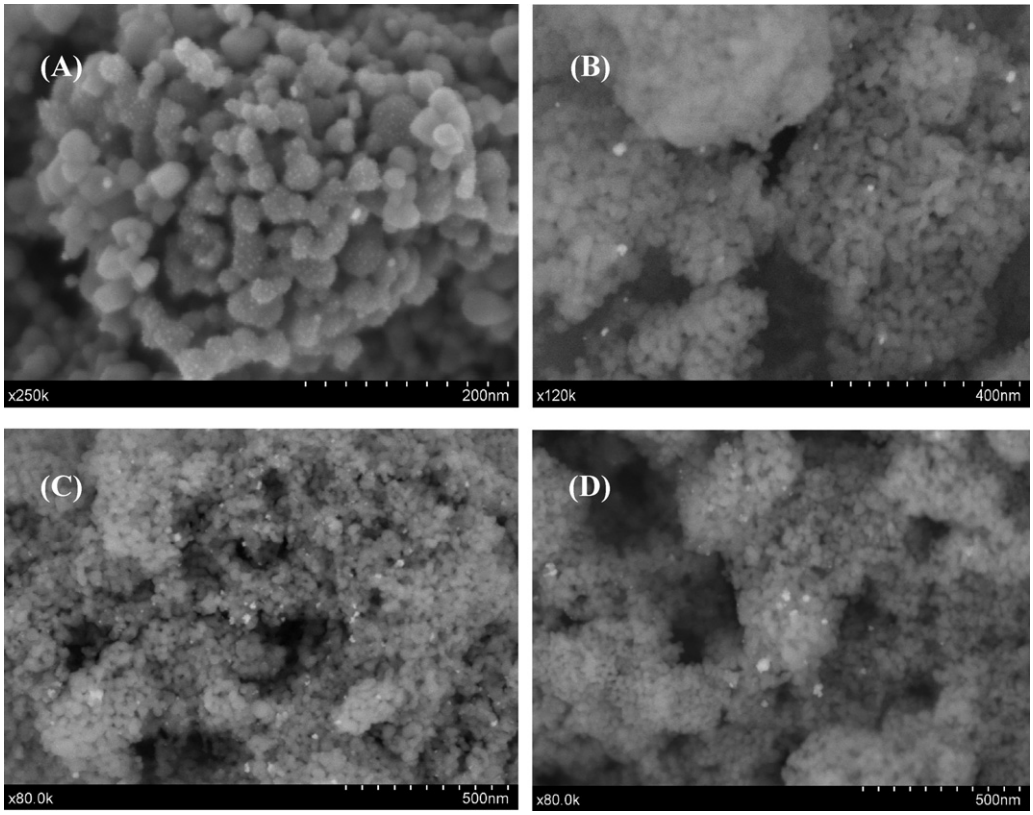

Fig. 3. SEM micrographs of Pt-TiO_2 samples prepared with different Pt loading and deposition time: 0.5 wt.% Pt-TiO_2 (A) 15 min and (B) 120 min; 2 wt.% Pt/TiO_2 (C) 15 min and (D) 120 min.

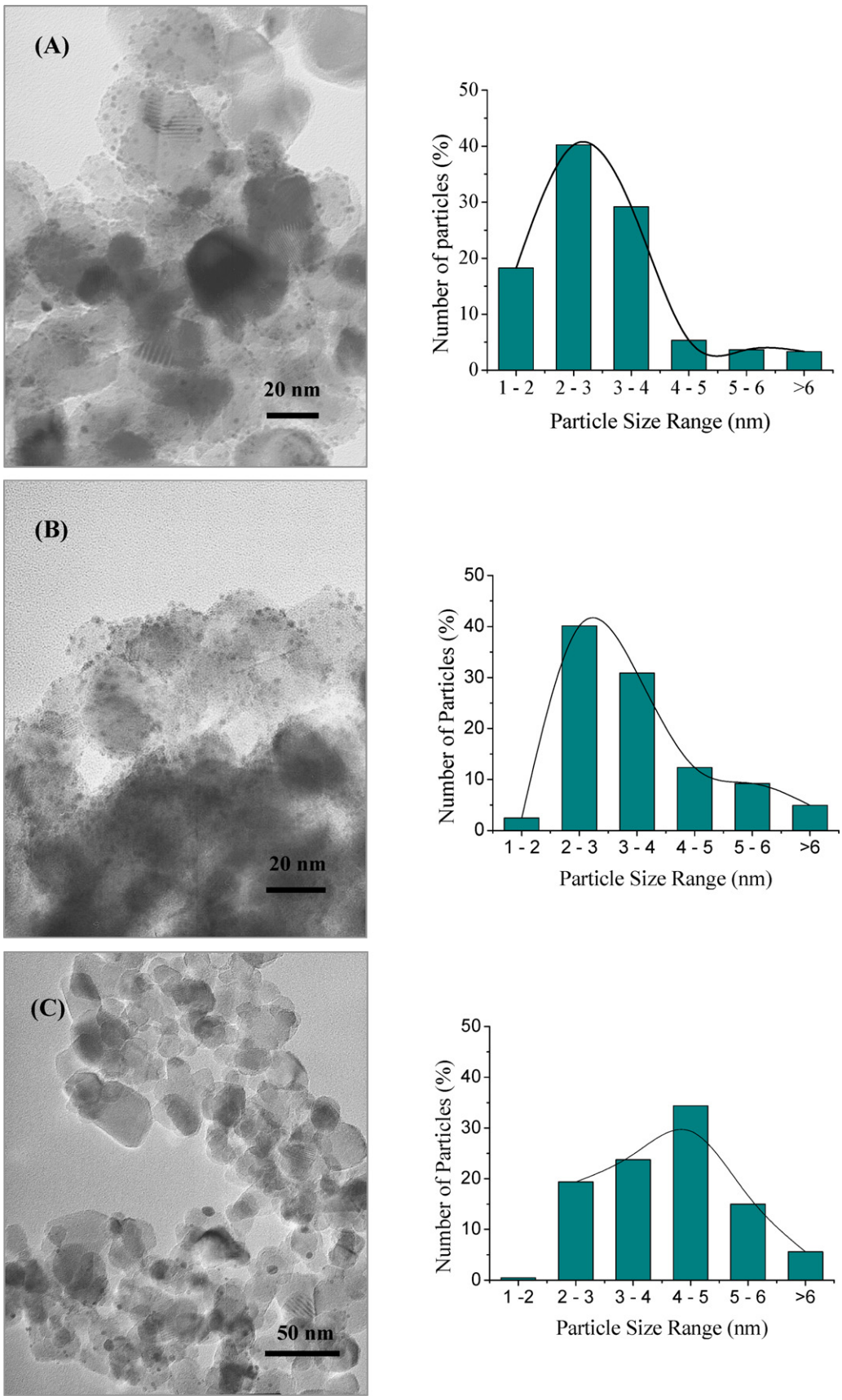

Fig. 4. TEM images and distribution of platinum particle size for 0.5 wt.% Pt-TiO_2 photocatalysts prepared with different deposition time: (A) 15 min; (B) 30 min; (C) 60 min; (D) 120 min and (E) 240 min.

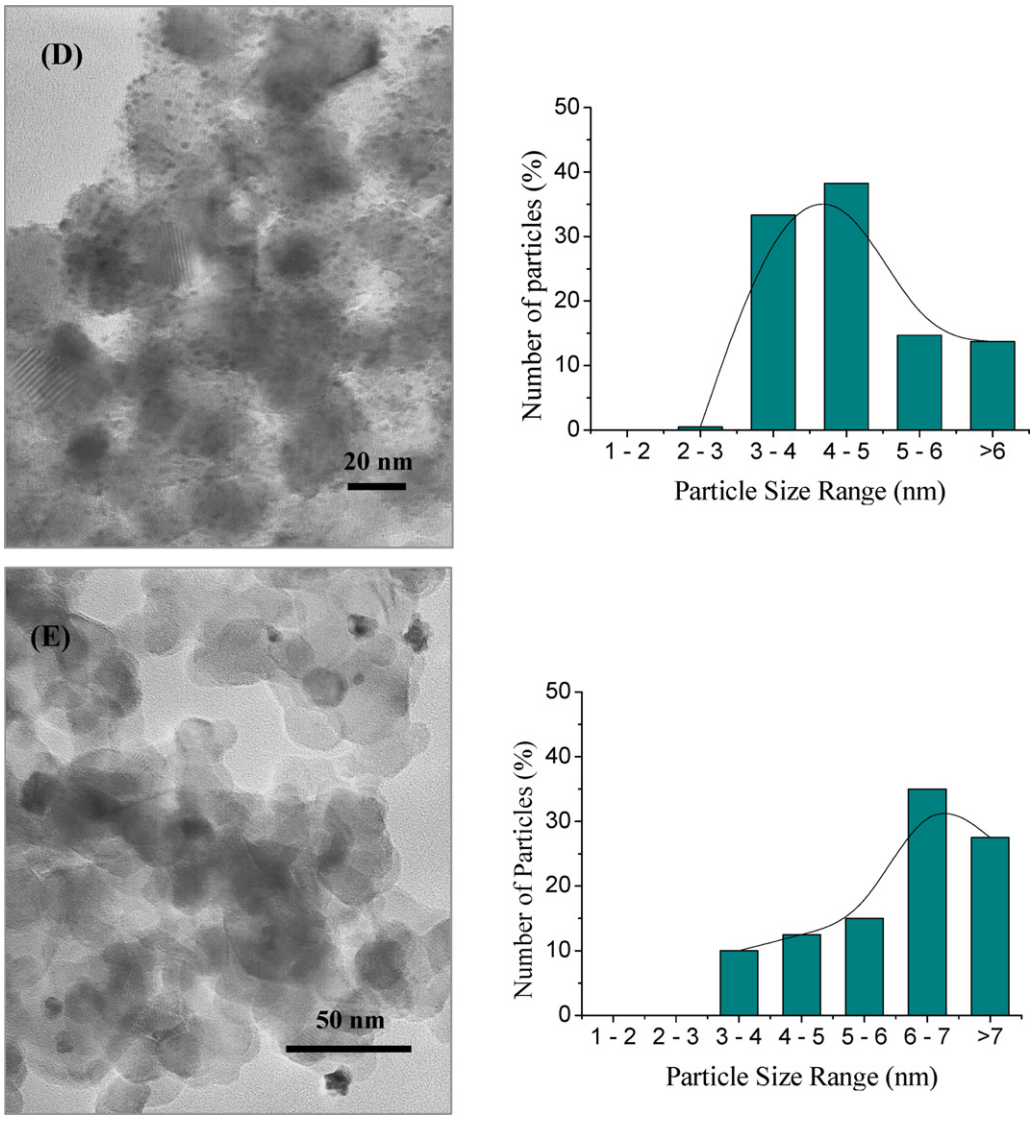

Fig. 4. (*Continued*).

particle sizes clearly increased with the deposition time. For 15 min the majority of metal particles are comprised between 2 and 3 nm, increasing progressively up to 240 min. For this time, the majority of particles are between 6 and 7 nm and additionally a high percentage of larger particle sizes is also found. It can also be observed a trend to form aggregations of the Pt particles for the longer deposition times, particularly for 240 min.

Photodeposition procedures reported in the literature have yielded metal deposits as small as a few nanometres or as large as several dozens of nanometres [3,5,20,26,32–34], proving the importance of choosing and controlling preparation conditions to obtained the desired properties of the materials. Moreover, this control appears crucial since size and dispersion of Pt deposits may have a direct influence on the photocatalytic properties of platinised TiO_2.

Average platinum particle diameter was calculated by using the equation described in the experimental section and the results are plotted in Fig. 5. As it can be seen, average diameter increased linearly with the deposition time in the studied time range. These results evidence that by controlling deposition time under these experimental conditions, the average size of Pt nanoparticles can be finely tuned.

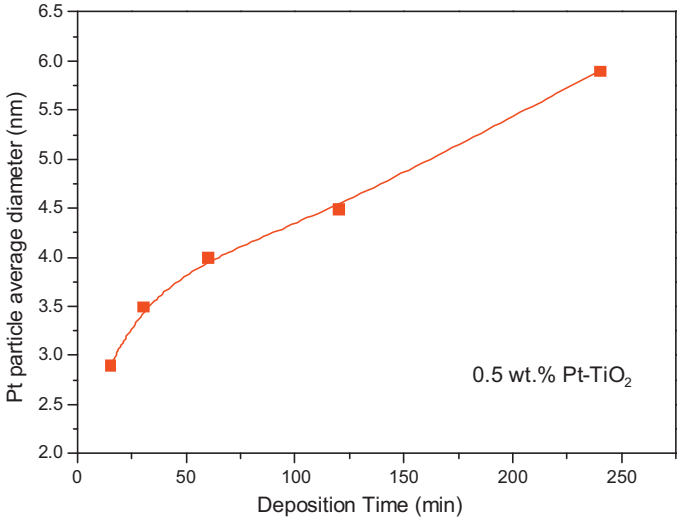

Fig. 5. Average platinum particle diameter for 0.5 wt.% Pt-TiO_2 samples as a function of deposition time.

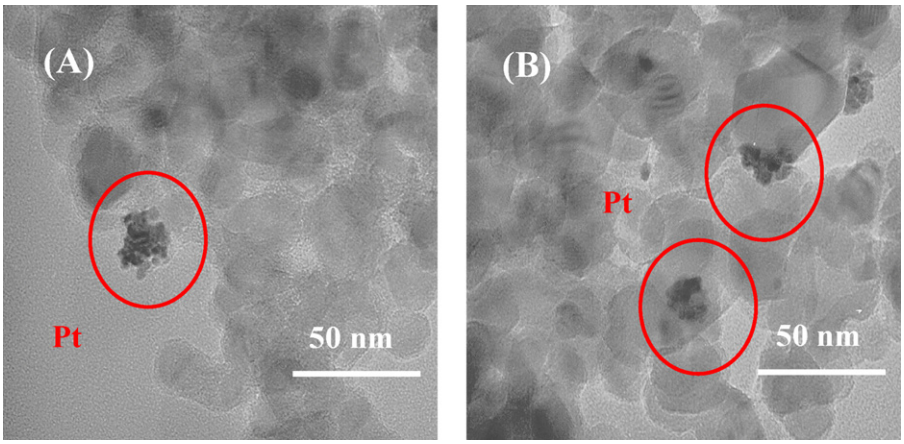

Fig. 6. TEM pictures for samples with 2 wt.% nominal Pt content, prepared with different deposition time: (A) 15 min and (B) 240 min.

Fig. 6 shows TEM pictures for samples with 2 wt.% nominal Pt content prepared with a short and a long deposition time, Fig. 6A and B respectively. It can be clearly seen that metal particles in these samples prepared with a higher metal loading are located heterogeneously forming clusters. Due to the aggregation of particles, performing the estimation of Pt particle size distribution in these samples was not possible. Nevertheless, as it can be qualitatively observed in the TEM images in Fig. 6 and in many others not shown, the size of individual Pt particles also increased with the deposition time.

Aggregation and growth of platinum particles with the deposition time and metal loading could be understood considering the mechanism of photodepositition for the metal reduction on the TiO_2 surface [23]. Platinum particles are nucleated on the TiO_2 surface with preferential deposition at oxygen vacancies where a high-electron density can be found. After reduction, platinum atoms have a valence electronic structure configuration s^1d^9 and with the adsorption and reduction on the oxygen vacancies, the empty orbitals of the metal atoms could be filled by the photogenerated electrons produced in the TiO_2, thus the electronic configuration of Pt could become the more stable s^2d^{10}. Reduction of new $[PtCl_6]^{2-}$ ions can only take place where photogenerated electrons arrive at the surface. The increased electron density on Pt atoms will hinder to a certain degree the creation of new nucleation sites on the TiO_2 surface and the reduction of the platinum precursor will take place preferentially over already adsorbed platinum on the surface making the deposits growth larger forming aggregates.

3.3. Pt chemical state

XPS analyses were performed for all the samples. The Ti $2p_{3/2}$ core level spectra were similar for the TiO_2 and the Pt-TiO_2 samples with peaks centred at binding energies 458.5 ± 0.1 eV, corresponding to Ti^{4+} in the TiO_2 network as the main component. Similarly, O 1s peaks were located at binding energies 529.8 ± 0.2 eV in all samples corresponding to lattice oxygen in TiO_2. These peaks were asymmetric (spectra not shown) with broad shoulders at higher binding energies ascribed to oxygen in surface hydroxyl groups. The shoulder was more pronounced in the platinised samples than in pure TiO_2, indicating a higher degree of hydroxylation in the former; however no significant differences among the samples prepared with different deposition times could be found.

O/Ti ratios estimated by XPS are presented in Table 1. The ratio for TiO_2 was found to be much lower than the stoichiometric value, indicating the presence of a certain amount oxygen vacancies on the surface. It has been reported that sulphate pre-treatment of

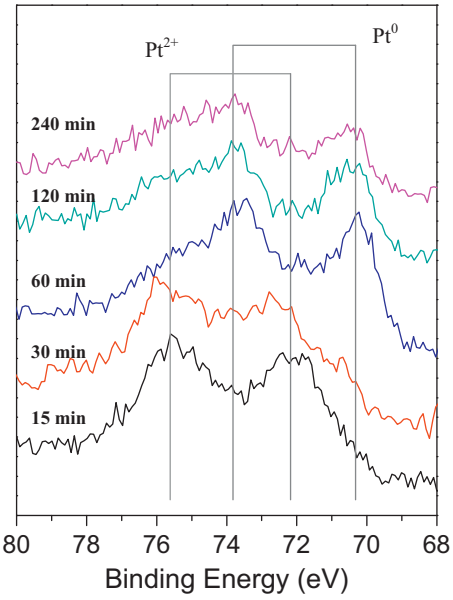

Fig. 7. XPS Pt 4f core level spectra for 2 wt.% Pt-TiO_2 catalysts prepared with the indicated deposition time.

TiO_2 and further calcination at relatively high temperature (650 °C) produces an oxygen vacant rich surface, which is a favourable circumstance for noble metal deposition [28]. As it can be seen in Table 1, O/Ti ratio increased to values close to 2 for the platinised samples, suggesting that the oxygen vacancies are partially annihilated during the photodeposition process, in agreement with previous results [28]. Oxygen from hydroxyl groups in the more hydroxylated surface of the platinised samples would also contribute to increase the O/Ti ratio.

The study of XPS Pt 4f peak region can provide information concerning the oxidation state of the Pt adsorbed species on the TiO_2 surface. In Pt-TiO_2 systems, the metal oxidation state is one of the factors with a stronger influence in the photocatalytic properties, being Pt^0 generally accepted as the state of platinum leading to most favourable results in photocatalytic activity [16]. Pt 4f region is formed by a doublet corresponding to the signals for $4f_{7/2}$ and $4f_{5/2}$. The Pt $4f_{7/2}$ binding energy for metallic platinum (Pt^0) appears near 70.5 eV while for oxidised forms (Pt^{4+}/Pt^{2+}) appears at higher binding energies with values ca. 74.5 and 72.5 eV, respectively [15].

XPS Pt 4f region for the Pt-TiO_2 samples with 2 wt.% metal content and prepared with the different deposition times is shown in Fig. 7. All the spectra were calibrated with the C 1s peak at

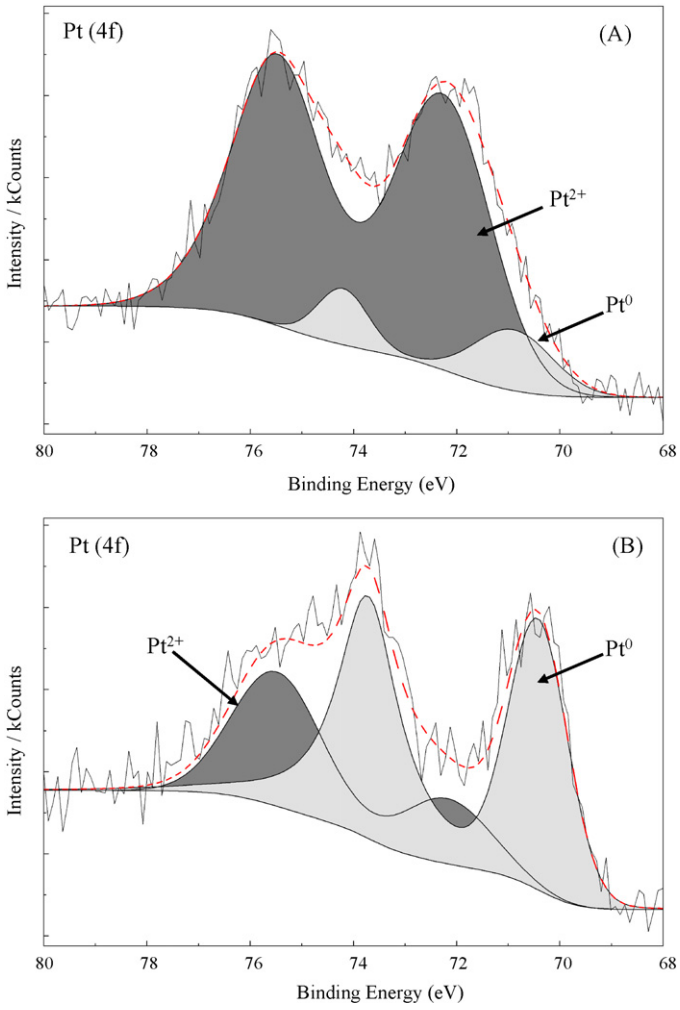

Fig. 8. XPS Pt 4f region for 2 wt.% Pt-TiO_2 samples prepared with different deposition times: (A) 15 min and (B) 120 min.

284.6 eV attributed to "adventitious" surface carbon. As it can be seen, platinum on the samples prepared with 15 and 30 min deposition time appears at binding energies which can be assigned to oxidation state 2+. Thus, H_2PtCl_6 precursor was not efficiently reduced for these short deposition times and the majority of the metal remained oxidised. On the contrary, for the samples prepared with longer deposition times, platinum can be undoubtedly assigned to metallic state, even though a certain contribution of Pt^{2+} can be also evidenced. In agreement with results reported by Kozlova et al. [26] the measured Pt $4f_{7/2}$ binding energy for these longer deposition times is slightly shifted to lower binding energies compared to typical bulk metallic platinum, suggesting electron transfer from the TiO_2 to the Pt which can be considered as an electron-rich state of the metal ($Pt^{\delta-}$).

Pt $4f_{7/2}$ and Pt $4f_{5/2}$ doublets were deconvoluted using the UNIFIT 2009 software [35] assuming a doublet separation of 3.3 eV of the two components. A Shirley type background was subtracted from each spectrum. In this analysis the Ti 3s signal with maximum around 63 eV, in the proximity to the Pt 4f region, was also taken into account. The deconvolution of the doublets gave us an estimation of the Pt^0/Pt^{2+} fractions in the different samples. As an example, Fig. 8 shows this deconvolution for the samples prepared with 15 and 120 min deposition time. The estimated fraction of metallic platinum as a function of the deposition time is shown in Table 1. As it can be seen, the fraction of Pt^0 increased notably with the deposition time up to 120 min, reaching a value of ca. 60%, and

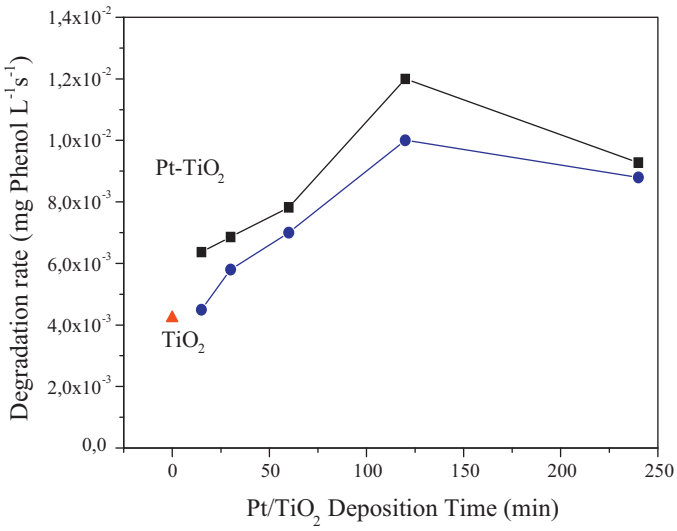

Fig. 9. Initial reaction rates for phenol photo-oxidation (milligram of phenol per litre and second) over Pt-TiO_2 photocatalysts as a function of Pt deposition time: (▲) TiO_2; (■) 0.5 wt. Pt/TiO_2; (●) 2 wt.% Pt-TiO_2.

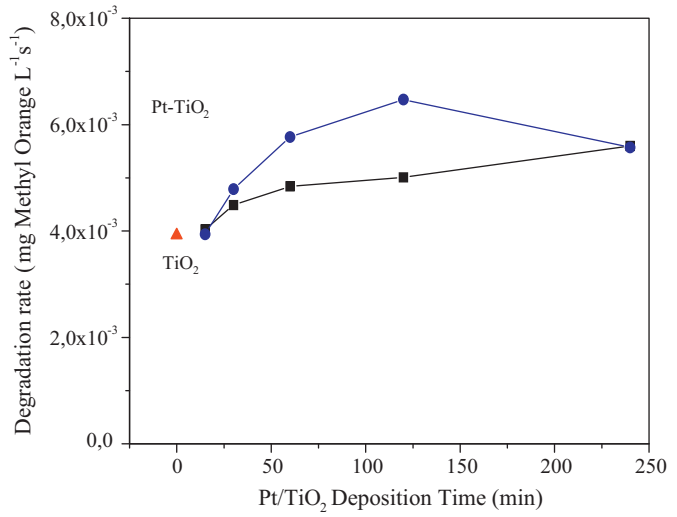

Fig. 10. Initial reaction rates for methyl orange photo-oxidation (milligram of methyl orange per litre and second) over Pt-TiO_2 photocatalysts as a function of Pt deposition time: (▲) TiO_2; (■) 0.5 wt. Pt/TiO_2; (●) 2 wt.% Pt-TiO_2.

then remained constant for the longer time of 240 min. It can be noted that the photodeposition process is not able to reduce the totality of the precursor for any deposition time, and it seems that the maximum fraction of Pt^0 that can be obtained is approximately 60%.

For the 0.5 wt.% Pt-TiO_2 series, Pt 4f XPS signal to noise ratio was too low to allow any accurate enough analysis of the region due to the low content of the metal. In any case, it could be assumed a similar trend than the one observed for 2 wt.% Pt-TiO_2 samples.

3.4. Photocatalytic activity

Photocatalytic activity was evaluated using the photooxidation of phenol and methyl orange in liquid media as test reactions. Values of the photodegradation rates for phenol and methyl orange oxidation are shown in Figs. 9 and 10 respectively.

For both tested reactions, the addition of Pt improved the photocatalytic efficiency of bare TiO_2 in higher or lower amount depending on the deposition time considered. For phenol

oxidation the activity increased gradually with the deposition time up to 120 min and then decreased for the longer deposition time of 240 min in both 0.5 and 2 wt.% Pt-TiO_2 samples. For methyl orange oxidation over the 0.5 wt.% Pt-TiO_2 the activity increased with the deposition time for all the studied times. Alike to phenol oxidation, methyl orange oxidation rate over 2 wt.% Pt-TiO_2 samples also increased up to 120 min and then decreased for the sample prepared with 240 min deposition time.

In the analysis of the activity results several parameters have to be considered. As it has been seen in the previous section, surface area, crystalline phase composition and light absorption properties are similar in the different samples and therefore no influence of these parameters on the activity should be expected. Besides, as it can be seen in Table 1, the amount of deposited Pt increased slightly up to 60 min deposition time and then stayed approximately the same (for both nominal Pt contents). S_{BET} also increased slightly up to 60 min and then decreased a little for longer deposition times. On the contrary, the activity increased in any considered case up to 120 min deposition time, with independence of the values of these parameters and therefore other arguments have to be considered.

The improvement in the photoactivity of TiO_2 by platinisation has been ascribed to the role of Pt deposits as electron wells thus inhibiting to a higher degree the recombination of photogenerated charge carriers. This will be theoretically more effective over small platinum deposits due to the higher surface area to volume ratio. However, according to our results, even more important than metal deposit size is the oxidation state of the metal. Platinum should be in its metallic form in order to allow the formation of a Schottky junction with the TiO_2 producing the above explained mechanism of enhancement. Thus, the activity for both tested reaction increased over the samples prepared with a deposition time up to 120 min, where a maximum in the Pt^0 fraction was observed. For longer deposition time (240 min) the fraction of metallic platinum remained approximately the same and then the larger average metal size surely made that the activity fell again. In this context, the insignificant improvement of the TiO_2 activity by photodeposition for 15 min, even though they presented the smallest size, can be understood by noticing that with this time platinum deposits are mainly in oxidised form.

Regarding the substrate to be degraded (phenol or methyl orange), same activity trend was found for both reactions. Thus, no important influence of the substrate was found, in contrast with other reported results [8,18,36] where the model reaction chosen for the activity tests appeared as a key factor for the improvement or reduction of the TiO_2 activity by platinisation.

On the contrary, the substrate plays a significant role in the influence of metal content on the activity. Thus, the activity for the series of samples with 0.5 wt.% nominal content of Pt is higher than for the series with 2 wt.% for phenol oxidation but the opposite can be observed for methyl orange degradation. This could be related to different adsorption properties of the samples depending on the metal loading together with different adsorption affinity of the two substrates which could favour the photooxidation of one or the other [37]. FTIR studies to elucidate this point are currently underway.

In conclusion, it becomes clear that information about platinum oxidation state and deposit sizes has to be always required for the understanding of photocatalytic properties of platinised systems.

4. Conclusions

The photodeposition of Pt on TiO_2 under different experimental conditions was performed and the photocatalytic activity of the obtained Pt-TiO_2 materials was evaluated by following the phenol and methyl orange oxidation reactions. Pt particle size could be precisely tuned by changing deposition time under medium light intensity during the photodeposition. Average platinum deposit size was increased from ca. 3 nm for 15 min to ca. 6 nm for 240 min deposition time. Platinum chemical state also depended strongly on the deposition time used during the photodeposition.

Photocatalytic activity results showed that platinum should be in its metallic state to produce an effective improvement of the activity regardless the size of Pt deposits (in the range 3–6 nm). When the fraction of Pt^0 was the same on the samples, the size of the metal deposit became the decisive factor for explaining the improvement of efficiency. Thus, it is always necessary to know platinum oxidation state and deposit sizes to compare and explain the photocatalytic properties of Pt-TiO_2 systems.

As often found in catalysis, a compromise of different factors has to be reached for the optimisation of the catalyst activity properties.

Acknowledgements

This research was financed by the Spanish Ministerio Ciencia e Innovación (Project Ref. CTQ2011-26617-C03-02). J.J. Murcia would like to thank CSIC for the concession of a JAE grant. CITIUS (University of Seville) is acknowledged for XPS and XRF measurements.

References

[1] A.A. Ismail, D.W. Bahnemann, Journal of Physical Chemistry C 115 (2011) 5784–5791.
[2] Z. Yu, S.S.C. Chuang, Applied Catalysis B: Environmental 83 (2008) 277–285.
[3] C. Millon, D. Riassetto, G. Berthome, F. Roussel, M. Langlet, Journal of Photochemistry and Photobiology A 189 (2007) 334–348.
[4] M.C. Hidalgo, M. Maicu, J.A. Navío, G. Colón, Journal of Physical Chemistry C 13 (2009) 12840–12847.
[5] V. Iliev, D. Tomova, L. Bilyarska, A. Eliyas, L. Petrov, Applied Catalysis B: Environmental 63 (2006) 266–271.
[6] A. Patsoura, D.I. Kondarides, X.E. Verykios, Catalysis Today 124 (2007) 94–102.
[7] S.G. Kumar, L.G. Devi, Journal of Physical Chemistry A 115 (2011) 13211–13241.
[8] J. Lee, W. Choi, Journal of Physical Chemistry B 109 (2005) 7399–7406.
[9] B.K. Vijayan, N.M. Dimitrijevic, J. Wu, K.A. Gray, Journal of Physical Chemistry C 114 (2010) 21262–21269.
[10] C.H. Huang, I.K. Wang, Y.M. Lin, Y.H. Tseng, C.M. Lu, Journal of Molecular Catalysis A: Chemical 316 (2010) 163–170.
[11] Y. Ishibai, J. Sato, T. Nishikawa, S. Miyagishi, Applied Catalysis B: Environmental 79 (2008) 117–121.
[12] S. Sakthivel, M.V. Shankar, M. Palanichamy, B. Arabindoo, D.W. Bahnemann, V. Murugesan, Water Research 38 (2004) 3001–3008.
[13] S.K. Lee, A. Mills, Platinum Metals Review 47 (2003) 61–72.
[14] V. Keller, P. Bernhardt, F. Garin, Journal of Catalysis 215 (2003) 129–138.
[15] A.V. Vorontsov, E.N. Savinova, J. Zhensheng, Journal of Photochemistry and Photobiology A 125 (1999) 113–117.
[16] W.Y. Teoh, L. Mädler, R. Amal, Journal of Catalysis 251 (2007) 271–280.
[17] L.A. Pretzer, P.J. Carlson, J.E. Boyd, Journal of Photochemistry and Photobiology A 200 (2008) 246–253.
[18] U. Siemon, D. Bahnemann, J.J. Testa, D. Rodriguez, M.I. Litter, N. Bruno, Journal of Photochemistry and Photobiology A 148 (2002) 247–255.
[19] F. Denny, J. Scott, K. Chiang, W.Y. Teoh, R. Amal, Journal of Molecular Catalysis A: Chemical 263 (2007) 93–102.
[20] M.C. Hidalgo, M. Maicu, J.A. Navío, G. Colón, Catalysis Today 129 (2007) 43–49.
[21] S. Hwang, M.C. Lee, W. Choi, Applied Catalysis B: Environmental 46 (2003) 49–63.
[22] S. Sato, Journal of Catalysis 92 (1985) 11–16.
[23] F. Zhang, J. Chen, X. Zhang, W. Gao, R. Jin, N. Guan, Y. Li, Langmuir 20 (2004) 9329–9334.
[24] M.C. Hidalgo, J.J. Murcia, J.A. Navío, G. Colón, Applied Catalysis A 397 (2011) 112–120.
[25] C.M. Ma, Y.W. Lee, G.B. Hong, T.L. Su, J.L. Shie, C.T. Chang, Journal of Environmental Sciences 23 (2011) 687–692.
[26] E.A. Kozlova, T.P. Lyubina, M.A. Nasalevich, A.V. Vorontsov, A.V. Miller, V.V. Kaichev, V.N. Parmon, Catalysis Communications 12 (2011) 597–601.
[27] B. Llano, G. Restrepo, J.M. Marín, J.A. Navío, M.C. Hidalgo, Applied Catalysis A 387 (2010) 135–140.

[28] M.C. Hidalgo, M. Maicu, J.A. Navío, G. Colón, Applied Catalysis B: Environmental 81 (2008) 49–55.
[29] S.P. Tandom, J.P. Gupta, Physica Status Solidi 38 (1970) 363–367.
[30] A. Baylet, C. Capdeillayre, L. Retailleau, J.L. Valverde, P. Vernoux, A. Giroir-Fendler, Applied Catalysis B: Environmental 102 (2011) 180–189.
[31] G. Colón, M.C. Hidalgo, J.A. Navío, Applied Catalysis B: Environmental 45 (2003) 39–50.
[32] H.T. Gomes, B.F. Machado, A.M.T. Silva, G. Dražić, J.L. Faria, Materials Letters 65 (2011) 966–969.
[33] S.W. Lam, K. Chiang, T.M. Lim, R.G. Amal, K-C. Low, Applied Catalysis B: Environmental 72 (2007) 363–372.
[34] D. Riassetto, C. Holtzinger, M. Messaoud, S. Briche, G. Berthomé, F. Roussel, L. Rapenne, M. Langlet, Journal of Photochemistry and Photobiology A 202 (2009) 214–220.
[35] University of Leipzig, Germany, www.uni-leipzig.de/~unifit.
[36] D. Hufschmidt, D. Bahnemann, J.J. Testa, C.A. Emilio, M.I. Litter, Journal of Photochemistry and Photobiology A 148 (2002) 223–231.
[37] C. Hu, Y. Tang, Z. Jiang, Z. Hao, H. Tang, P.K. Wong, Applied Catalysis A 253 (2003) 389–396.